Cyber-physical Modeling Technique based Dynamic Aggregation of Wind Farm Considering LVRT Characteristic

Guiqing Ma, Yunlu Li, Junyou Yang, *Member, IEEE,* and Bing Wu

Abstract—**With the increasing penetration of wind power, large-scale integrated wind turbine brings stability and security risks to the power grid. For the aggregated modeling of large wind farms, it is crucial to consider low voltage ride-through (LVRT) characteristics. However, in aggregation methods, the approximate neglect behavior is essential, which leads to inevitable errors in the aggregation process. Moreover, the lack of parameters in practice brings new challenges to the modeling of a wind farm. To address these issues, a novel cyber-physical modeling method is proposed. This method not only overcomes the aggregation problem under the black-box wind farm but also accurately realizes the aggregation error fitting according to the operation data. The simulation results reveal that the proposed method can accurately simulate the dynamic behaviors of the wind farm in various scenarios, whether in LVRT mode or normal mode.**

Index Terms—**Wind farm, Aggregated model, Low voltage ride through, Operation data.**

I. INTRODUCTION

WITH the advance in renewable energy generation, the proportion of wind energy in the power grid is increasing. The integration of large-scale wind power brings stability and security risks. Therefore, it is essential to build an accurate wind farm equivalent model for transient stability analysis and risk reduction. At present, the clustering-based aggregation method is the mainstream to study large-scale wind farms, which are generally classified as single-machine or multi-machine aggregation [1]-[2]. The single-machine aggregation model is too idealized to accurately represent the dynamic behavior of wind farms [3]-[4]. In contrast, more reasonable clustering criteria for multi-machine aggregation can achieve more accurate behavior expression.

In the multi-aggregation method, wind direction, wind speed, and equivalent power angle are often regarded as the main clustering criteria. In [5]-[6], wind turbines with the same or similar wind speeds are aggregated together. The method in

Guiqing Ma, Yunlu Li, Junyou Yang and Bing Wu are with the School of Electrical Engineering, Shenyang University of Technology, Shenyang, 110870, China (e-mail: guiqingm@126.com; liyunlu@sut.edu.cn; junyouyang@sut.edu.cn; wbing0824@126.com).

[7]-[8] classifies and aggregates wind farms according to turbine types and configuration, but their methods are mainly applicable to power quality analysis. A geometric template matching-based time series aggregation method is proposed in [9], which considered the wind speed and the layout of wind farms. However, the low voltage ride-through (LVRT) characteristics of wind turbines are not considered in the above method.

Wind turbines are sensitive to voltage sags, sudden transient fault can seriously affect its dynamic response [10]. LVRT mode is the key to ensuring the stable operation of wind farms under abnormal grid conditions [11]. However, whether the wind turbine enters the LVRT mode depends on the wind speed before the grid fault, the severity of the grid fault and many other factors. In [12]-[13], an aggregation method based on a crowbar circuit is proposed, which judges whether the wind turbines enter the LVRT mode according to the voltage drop at the bus terminal. However, different wind turbines on the same busbar, even under the same voltage sag depth, may lead to different states due to different wind speeds. An equivalent method for doubly fed induction generation (DFIG) based on density peak clustering algorithm is proposed in [14]. In [15], the wind speed combination model based on LVRT is described, which is used as the criteria for aggregate modeling. In [16], a two-machine aggregation method considering the fault ride through (FRT) process is proposed. However, there are inevitable errors in aggregation modeling. Trade-offs are usually needed between accurate models and complex aggregation criteria. Especially in LVRT mode, it is difficult to ensure the accuracy of LVRT characteristic expression under simplified aggregation criterion.

To establish the aggregation model of a wind farm, the detailed parameters of wind turbines are essential regardless of clustering criteria. However, all the above aggregation methods are based on the acquisition of all the detailed parameters. in practice, due to property rights protection or equipment aging and other factors [17], the obtained parameters are not accurate and even some wind turbine parameters cannot be obtained. However, all the above aggregation methods are based on the acquisition of all the detailed parameters. in practice, due to property rights protection or equipment aging and other factors, the obtained parameters are not accurate and even some wind turbine parameters cannot be obtained. This leads to the entire wind farm becoming a black box dynamic system.

In recent years, the rapid development of data-driven has been widely used in various fields [18]. Data-driven provides a powerful nonlinear modeling method that can generate complex nonlinear models from data. Due to this advantage, data-driven technology is widely used in many projects, such as energy management [19], Monitoring data classification [20], Behavior Prediction [21], etc. However, the data-driven model requires a large amount of data support to achieve high precision. To make up for this defect, a cyber-physical driven system is proposed. It reduces the amount of data required for model training based on prior knowledge. Therefore, cyber-physical systems have more structural advantages when addressing large-scale systems such as wind farms.

Aiming at the above problems, to accurately consider LVRT characteristics in wind farm aggregation modeling with unknown parameters, a cyber-physical technique modeling method is proposed in this paper. In this method, a cyber-driven model is constructed with neural network technology to correct the error between the aggregation model and the operating data. Due to the existence of the error compensation model, in the physical drive part, those turbines with unknown parameters can be replaced by the neural network equivalent model. Moreover, the operation data truly reflects the operation status of each wind turbine in the system, which can more accurately reflect the LVRT characteristics. Case studies under a wide range of multiple operating points demonstrate its accuracy. The contributions are as follows.

(1) It not only solves the aggregation challenge brought by the lack of wind turbine information in practice, but also considers the dynamic response characteristics of different fans under LVRT mode switching.

(2) A novel cyber-physical modeling framework is proposed，which incorporates the prior information and takes advantage of the data-driven. The advantages of the proposed framework are demonstrated under multiple operating points.

The remainder of this paper is organized as follows. The modeling of DFIG considering LVRT mode is presented in Section II. In Section III, the key points of aggregation modeling and neural network construction are discussed in detail. In Section IV, the performance evaluation of the proposed method under multiple operating conditions is presented. Section V concludes the paper.

II. MODELING OF DFIG CONSIDERING LVRT CAPABILITY

The typical DFIG structure is shown in Fig. 1. The rotor is integrated with the grid through the grid side converter and the rotor side converter, and the two converters are connected through the DC link. By controlling the crowbar circuit to achieve LVRT characteristics, the detailed mathematical model of DFIG can be found in [22].

It is clear from the [23] that although the LVRT processes of different wind farms are different, their dominant dynamics are almost the same. In LVRT mode, the power response curve is shown in Fig. 2. It can be seen from Fig.2 that when a grid fault occurs, the crowbar circuit acts quickly and switches the DFIG to the LVRT mode. After a short transient, both the active

power and the reactive power quickly tend to be stable. After fault clearance, the active power returns to the steady state at a certain rate, and the reactive power returns to the steady value immediately. The whole process is divided into three stages: steady state, fault and recovery. The active and reactive power are as follows.
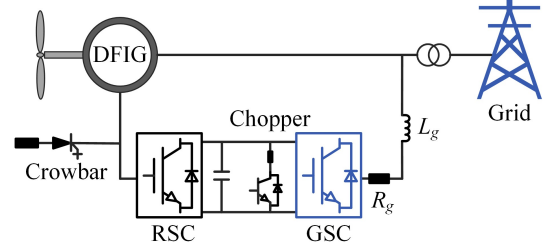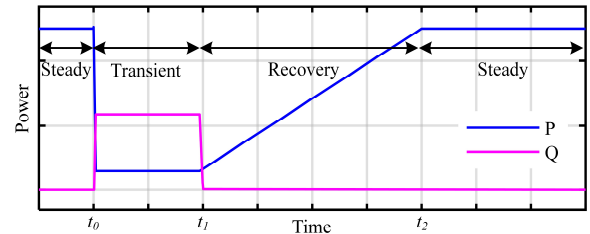

Fig. 1. The typical DFIG structure.

Fig. 2. General power response during the LVRT process.

$$P = \begin{cases} P_{state} & (t \le t_0, t > t_2) \\ P_{fault} = 0 & (t_0 < t \le t_1) \\ P_{recovery} = k_{rp}(t - t_1) + P_{fault} & (t_1 < t \le t_2) \end{cases} \quad (1)$$

$$Q = \begin{cases} Q_{state} & (t \le t_0, t > t_2) \\ Q_{fault} = k_{rq}(t - t_1) & (t_1 < t \le t_2) \end{cases} \quad (2)$$

where k_{rp} and k_{rq} are the LVRT coefficients for active and reactive powers, respectively.

According to the basic dynamic response curve requirements shown in Fig. 2, a detailed transient simulation model of DFIG is built. The control strategy and detailed parameter settings of the LVRT model are used in this paper as follows [24].

1) In the steady phase ($t \le t_0$), the crowbar circuit with a resistance of 0.1Ω is connected to the rotor for 60ms after a fault is detected.

2) In the fault phase ($t_0 \le t \le t_1$), the reference values of reactive power and active power are set to 0.2 and 0p.u, respectively.

3) In the recovery phase ($t_1 \le t \le t_2$), the active power recovery rate is set to 0.2p.u. per second.
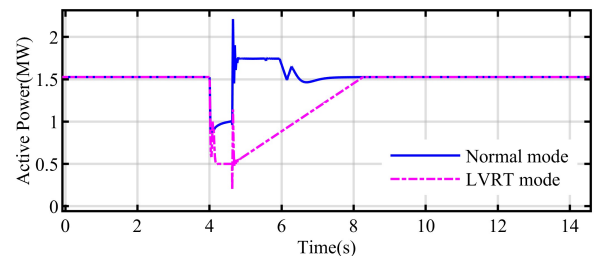

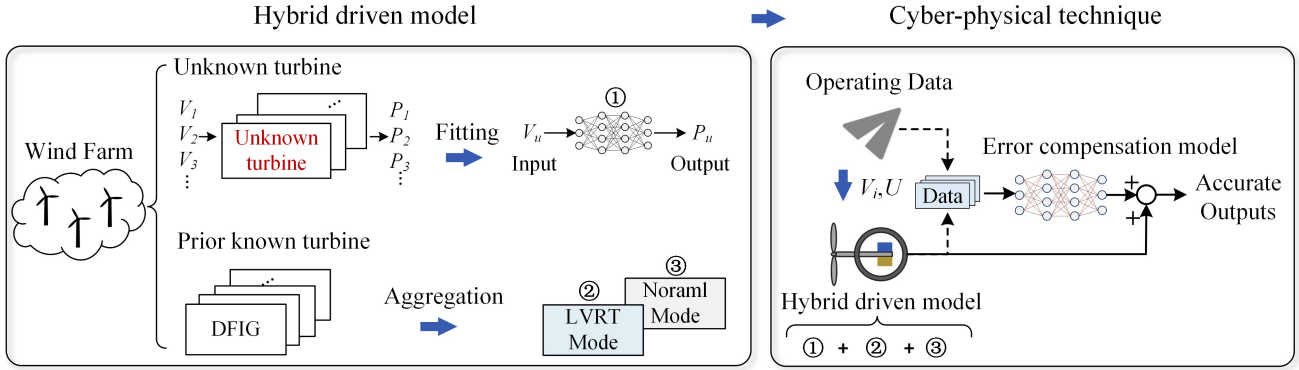Fig. 3. LVRT dynamic response of a single DFIG wind turbine generator.

Fig. 4. General framework of the proposed cyber-physical method.

According to national grid regulations, the dynamic response of wind turbines entering LVRT mode is different from that in normal mode, especially for DFIG [25]. Fig. 3 shows the dynamic response comparison of a single DFIG under LVRT mode and normal mode under grid fault. It can be seen that whether the wind turbine enters the LVRT mode has a significant impact on the dynamic response, so it is necessary to consider whether the wind turbine enters the LVRT mode during aggregation.

III. DYNAMIC AGGREGATION MODELING OF WIND FARM CONSIDERING LVRT CHARACTERISTICS

Due to the detailed parameters of each wind turbine cannot being obtained in practice, the wind farm system becomes a black-box dynamic system. The LVRT characteristics of the black-box system make the aggregation modeling extremely complex. To solve this special issue, the proposed cyber-physical modeling method is studied in this section. Fig. 4 illustrates a general framework of applying the cyber-physical method to realize aggregation of wind farms with unknown parameters in LVRT mode. The framework is organized with two parts, which are hybrid driven part and cyber-physical part. The hybrid driven part is composed of two steps. The first step is established the mapping model of wind turbines with unknow information. Then, clustering is performed according to whether the wind turbine enters the LVRT mode. The hybrid driving model is formed by combining the clustering model with the mapping model. In the cyber-physical part, the error between the aggregation model and operating data is compensated by error compensation model. More detailed principle of two part is explained as the follows.

A. Characteristic Fitting of Wind Turbines with Unknown Information

Regardless of the clustering criteria, building an aggregated model of a wind farm with detailed parameters is essential. Therefore, the first step of the aggregation is to establish the mapping model of the black-box wind turbines.

Due to the wind farm monitoring system, we can typically get the wind speed of each unit and the total power of the wind farm. To make full use of the prior information, this paper proposes an unknown turbine mapping method as shown in Fig. 5. The wind speed-power mapping model of the unknown unit

is obtained by iterative training.

To obtain the mapping model of the unknown turbine, the input should be obtained first. The wind speed of the unknown turbine is obtained through the wind farm monitoring system, and the sum is input to the neural network as the input. The total power of the unknown turbine is used as the iteration criterion. After iterative training, the overall wind speed-power characteristics can be obtained, as shown in Fig. 6. Based on these characteristics wind speed aggregation is carried out.
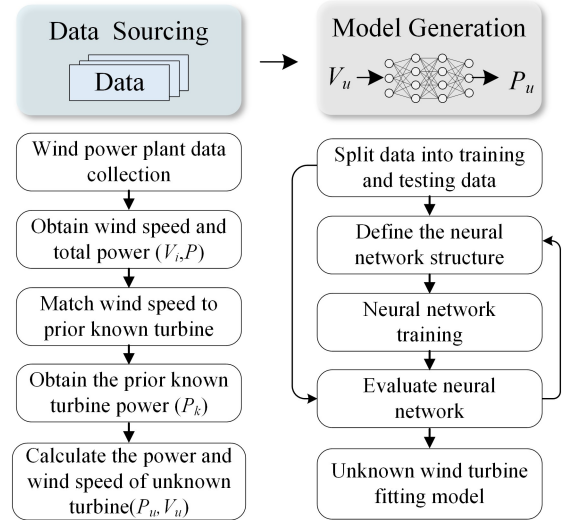

Fig. 5. Schematic diagram of fitting the unknown turbine characteristic.
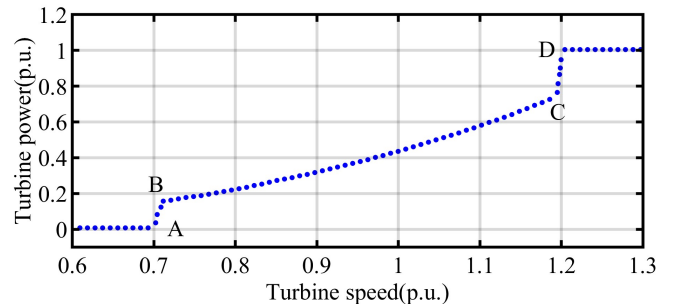

Fig. 6. The wind speed-power mapping relationship of the unknown turbine.

Wind speed aggregation is a necessary step for the clustering model. In this section, wind data of wind farms in eastern China is considered. It contains the wind speed and active power of all wind turbines in 2015 for the two wind farms. 20 wind turbines of data were randomly selected for preprocessing. Data sets

with missing data or abnormal data are discarded. In addition, to ensure that DFIG is in working mode, only the dataset with wind speed exceeding 5 m/s is retained. Since the power curves of all wind turbines were obtained in the previous step, the equivalent wind speed V_{eq} can be calculated by

$$V_{eq} = \sum_{j=1}^{N} f_j^{-1} \left(\frac{1}{S} \sum_{i=1}^{S} P_i \right) \tag{3}$$

where S denotes the number of aggregated wind turbines with the same power characteristics, N denotes the number of types of power characteristics, P_i and f^1 represent the active power of the i-th wind turbine and the inverse function of the wind turbine power curve, respectively.

B. Aggregation Modeling Method Based on LVRT

The next step is wind turbine aggregation. From the analysis in Section II, it can be seen that whether to enter the LVRT mode has a significant impact on the dynamic responses. Therefore, in this paper, the whole wind farm is aggregated into two units according to whether to enter LVRT mode. According to the operating data of the wind farm, the direct relationship between wind speed, terminal voltage drop depth, and whether a single DFIG enters the LVRT mode is plotted, as shown in Fig. 7. The aggregation according to this standard. The schematic of the aggregation is shown in Fig. 8. It contains 20 wind turbines on 2 busbars. The detail parameters of A3, B3, and B7-B9 are unknown. In the aggregation, the wind turbines with unknown parameters are replaced by the neural network. The aggregation method follows the existing method, which is the capacity-weighted method [26]. The aggregation process includes the equivalent parameters of DFIG, shafting and collector lines. The process is expressed as Eq. (4) to Eq. (6).

$$\begin{cases} S_{eq} = \sum_{i=1}^{n} S_i, P_{eq} = \sum_{i=1}^{n} P_i, R_{seq} = \sum_{i=1}^{n} \frac{R_s}{n}, R_{req} = \sum_{i=1}^{n} \frac{R_r}{n} \\ X_{seq} = \sum_{i=1}^{n} \frac{X_s}{n}, X_{req} = \sum_{i=1}^{n} \frac{X_r}{n}, X_{meq} = \sum_{i=1}^{n} \frac{X_m}{n} \end{cases} \tag{4}$$

$$\begin{cases} H_{teq} = 1/S_{eq} \sum_{i=1}^{n} H_{ti}S_i \\ H_{geq} = 1/S_{eq} \sum_{i=1}^{n} H_{gi}S_i \\ K_{seq} = 1/S_{eq} \sum_{i=1}^{n} K_{si}S_i \end{cases} \tag{5}$$

where n is the number of units on the same bus, S and P are the capacity and active power of the DFIG, respectively. R_s, R_r, L_s, and L_r are the resistance of stator and rotor, the inductance of stator and rotor. L_m is the magnetizing inductance. H_t, H_g, and K_s are inertia time of wind farm and generator rotor, and stiffness coefficient of shafting, respectively.

The equivalent representation of the collector network is also a crucial step. Since the connection between the impedance of the collector network in the wind farm and the wind turbines is not a pure parallel connection, it is unable to quickly estimate the transient depth of each wind turbine. In [27], a conversion method is proposed to convert several units on a single feeder into several units connected to PCC in parallel. The

transformation process is shown as.

$$Z'_{eqi} = \frac{Z_i \| Z'_{i-1}}{(Z_i \| Z'_{i-1}) + Z_{li}}, Z_{eqi} = \prod_{j=i}^{N} Z'_{eqi} \tag{6}$$

where Z_{eqi} is the equivalent impedance of the line connecting the i-th wind turbine directly to the PCC, $Z'_0 = \infty$.
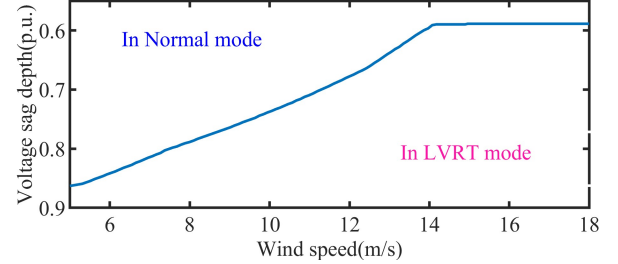

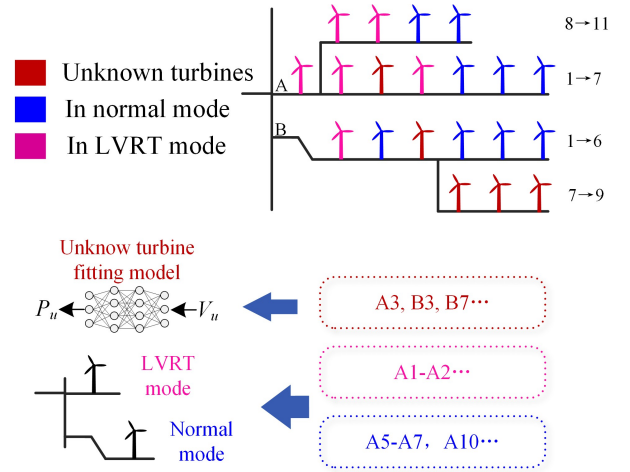Fig. 7. Condition for LVRT enabled and disable mode of a DFIG.

Fig. 8. The schematic of the aggregation.

C. Cyber-physical Hybrid Driven Frame

Due to the unavoidable behavior of approximate neglect in the process of aggregation, such as wind speed aggregation, line transformation, wind turbine equivalence, etc. The dynamic characteristics of the aggregation model are always inconsistent with the real wind farm. Most aggregation methods perform well in the steady state, but the accuracy is obviously decreased under big faults, especially after triggering LVRT mode.

Focus on this special problem, a cyber-physical hybrid-driven framework is proposed in this paper. Fig. 9 illustrates a general framework for applying the method. The working principle of the hybrid drive framework can be described below. Firstly, the operation data of wind farm buses at different operating points (P, Q, U_g) and the real-time wind speed (V_i) are collected. Then, the aggregation model is configured according to the wind speed and terminal voltage to ensure that it works at the same operating point. A large amount of power data with error information are obtained by simulation under different operating conditions. The output data (P_{agg}, Q_{agg}) of the aggregation model and operating data are taken as the input of the neural network, and the error data are taken as the target output. Finally, through the training of the network, the output value is as much as possible to fit the power error.
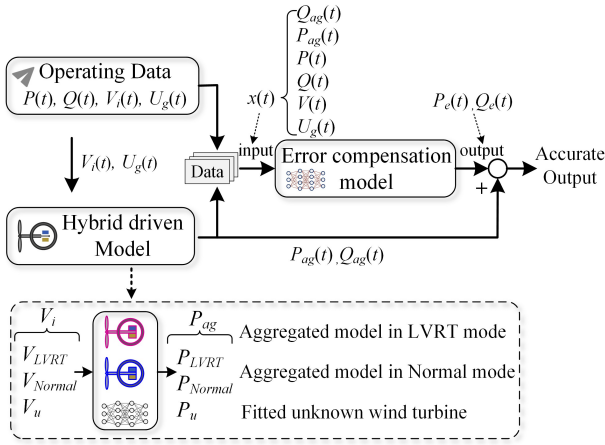
Fig. 9. Overall architecture of the cyber-physical method.

For the design of a neural network, the selection of neuron types is often the first step. Various types of neuron types have been described in [28]. The selection of neuron types depends on the type of modeling task, error fitting is a regression task that generates a model from measurement data. RNN neurons are often used for regression tasks. Although the RNN is feasible in theory, it suffers from gradient vanishing or exploding in the training process [29]. Hence, the LSTM-based RNN is selected to solve these drawbacks in this paper.

After determining the type of neurons, the next step is the design of the network structure. In a neural network, there are two categories of parameters, the weights and biases are automatically determined in the training process, and the hyperparameters need to be manually adjusted according to the task studied. The complexity of the studied tasks is a key factor in determining the number of neurons. In addition, adding normalization calculation in the network is an effective means to speed up the convergence, which can transfer the input data to 0~1 according to the maximum and minimum values of each feature sequence. The effect of the BN layer is similar to normalization. Based on the above considerations, the network structure is shown in Fig. 10.
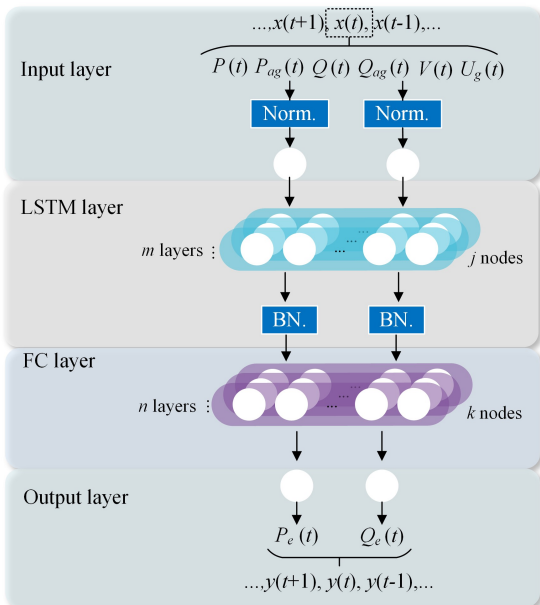

Fig. 10. The structure of the neural network.

IV. CASE STUDY

In this section, the proposed Cyber-physical technique is applied to black-box aggregate modeling of wind farms considering LVRT characteristics. The simulation was conducted in Matlab/Simulink environment. TensorFlow is used for building neural networks. The whole studies are performed on Intel Core i9-10900K CPU.

A. Configuration Setup

The proposed method is implemented on a wind farm with 20 DFIG turbines, as shown in Fig. 11. The installed capacities of each DFIG turbine are 1.5MW at rated wind speed. The total installed capacity is 30MW and the rated voltage of the collection network is 35kV, the nominal frequency is 50Hz. The impedance parameters of the network are set as R_{line}=0.16Ω/km, X_{line}=0.26mH/km. The detailed parameters for wind turbines are shown in Table I. To reflect the randomness of wind speed, the wind speeds of 20 wind turbines under 12 scenarios are randomly selected, as shown in Fig. 12. Faults occur in random scenarios. Short-circuit faults occur randomly in the range of 15Ω to 1 Ω. Considering the complexity of the studied wind farm, the hyperparameters of the proposed neural network are determined by repeated testing. Based on the structure in Fig. 9, the overall structure consists of two LSTM layers and two FC layers (m=2, n=2). Each LSTM layer has 128 neurons and each FC layer has 128 neurons (k=128, j=128).
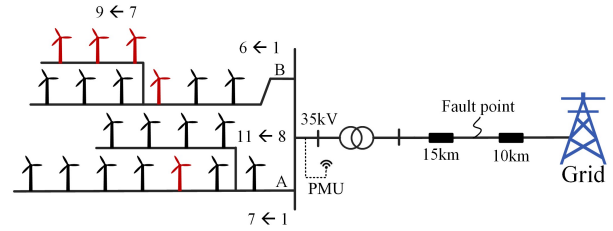

Fig. 11. Layout of the testing system.

TABLE I
PARAMETERS OF WIND TURBINES

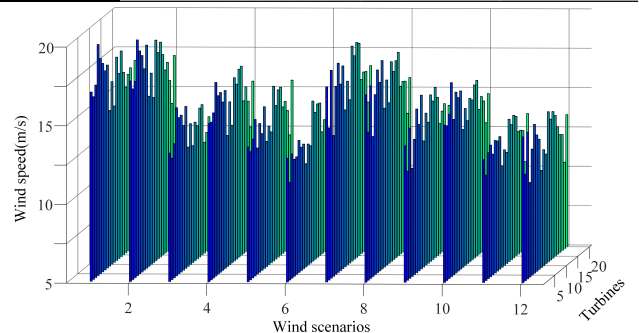|		A1-2,4-7	A8-11	B1-2,4-6
DFIG	R_s (p.u.)	0.00706	0.0088	0.0072
	R_r (p.u.)	0.005	0.007	0.007
	L_s (p.u.)	0.171	0.18	0.17
	L_r (p.u.)	0.156	0.167	0.14
	L_m (p.u.)	2.9	6.22	3.0
	H_t (s)	4.32s	5.2s	4.32s
	H_g (s)	0.5s	0.5s	0.72s
	K_s (p.u.)	1.11	1.05	1.11
Grid-side converter	k_{gp}	1	2	2
	k_{gi}	100	150	150
Rotor-side converter	k_{rp}	0.3	0.05	0.05
	k_{ri}	8	5	5

Fig. 12. Twelve wind scenarios randomly selected from real wind data from actual wind farms.

The mean-square error (MSE) is used to evaluate the fitting performance of the trained network on the training procedure. The MSE calculation process is as follows.

$$\text{MSE} = \frac{1}{N}\sum_{i=1}^{N}(y_i - \hat{y}_i) \qquad (7)$$

where y_i and $\hat{y}_i$ represents the actual and fitted values, respectively. N is the total number of time steps. After 4000 iterations, the MSE of training data and validation data decreased to 0.01, which indicates that the trained network can accurately fit the error of the aggregation model.

B. Dynamic Response Analysis

As discussed in Section III, aggregation of wind turbines is based on whether the wind turbine enters the LVRT mode or not. With the help of the wind turbine numbers shown in Fig. 11, Table II shows the operating state of the wind turbines at different voltage sag levels.

TABLE II
OPERATING CONDITIONS OF EACH WIND TURBINE

Voltage sag depth	LVRT mode	Wind turbine Groups
-0.17 p.u.	Yes	A1-2, A4-11, B1-2, B4-6
	No	---
-0.59 p.u.	Yes	A1-2, A8-9, B1-2
	No	A4-7, A10-11, B4-6
-0.76 p.u.	Yes	A1-2, A4-6, A8-10, B1-2
	No	A7, A11, B4-6

In this section, the proposed cyber-physical hybrid-driven method is validated in multiple operating points and severe disturbances. In the first scenario, as shown in Fig. 13, the wind farm is exporting 20 MW active power. The three-phase short-circuit fault at the transmission line occurs in 2s and lasts 1.25s with a 10Ω short circuit resistance. Due to this fault, the voltage at PCC drops to 0.83p.u. As shown in Fig. 7, the activation of LVRT mode is determined according to the wind speed and terminal voltage drop. According to the curve, the turbines without entering LVRT model.

As shown in Fig. 13, in normal mode, the peak errors of the active and reactive power of the aggregation model under 10Ω grounding resistance are 0.48% and 0.37%, respectively. After
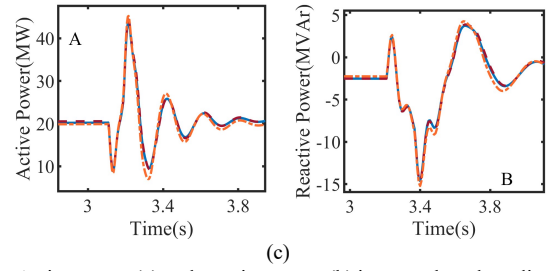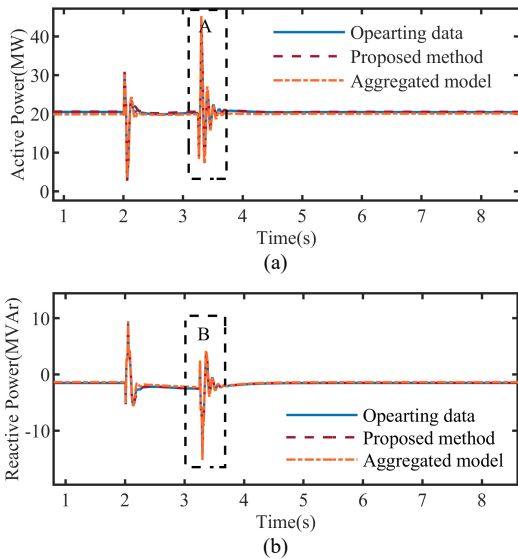

(a)

(b)

(c)

Fig. 13. Active power (a) and reactive power (b) in normal mode at disturbance occurs (three-phase short-circuit fault with 10Ω).

the intervention of error compensation model, the errors decreased to 0.05% and 0.04%, respectively.

In scenario 2, 2Ω grounding fault occurs at fault point, and the voltage of PCC drops to 0.41p.u. Fig.14 shows the proposed method in LVRT model. In Fig.14, wind farm outputs 25MW active power, the fault occurs in 4s lasts 0.625s. The peak error is 3.26% for active power and 2.58% for reactive power in aggregation model. In contrast, the peak error of active power is only 0.16% and 0.15% for reactive power in the proposed method.
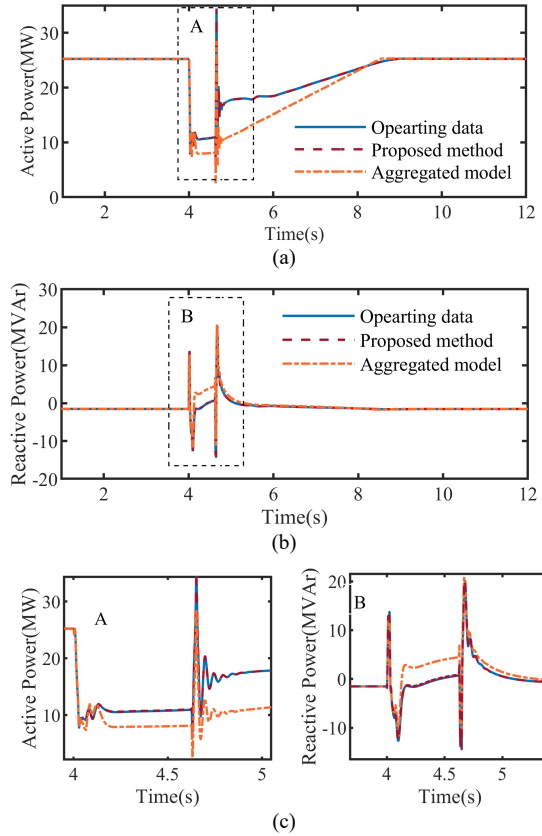

(a)

(b)

(c)

Fig. 14. Active power (a) and reactive power (b) in LVRT mode at disturbance occurs (three-phase short-circuit fault with 2Ω).

In scenario 3, the proposed method implemented with 0.8Ω ground resistance. The fault occurs at 4s lasts 0.625s, and the PCC voltage drops to 0.24p.u. With fault impedance. The corresponding curves are presented in Fig. 15. The peak error of active power and reactive power is 1.62% and 2.38% in the aggregation model. By contrast, the error of the proposed method is only 0.18% for active power and 0.15% for reactive power.
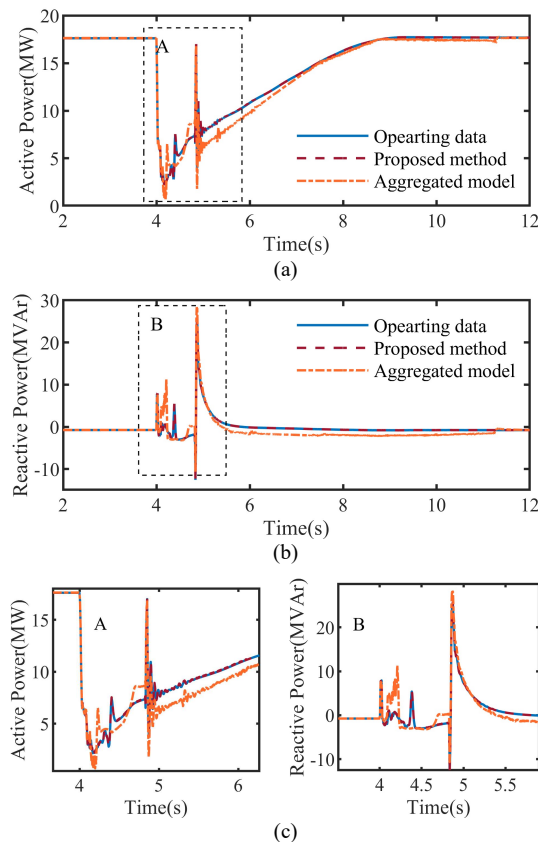
Fig. 15. Active power (a) and reactive power (b) in LVRT mode at disturbance occurs (three-phase short-circuit fault with 0.8Ω).

To more intuitively compare the error of active power and reactive power response, the mean absolute errors (MAEs) is used as an index to visualize the modeling accuracy. The associated MAEs are shown in Table III. It can be seen from Table III that the error of the proposed method in the whole dynamic process are substantially smaller than the traditional method, especially under LVRT mode. The comparison results demonstrate the proposed hybrid drive method can accurately realize the dynamic equivalent modeling of wind farms with unknown parameters, whether in LVRT mode or normal mode.

TABLE III
ERROR COMPARISON OF ACTIVE POWER AND REACTIVE POWER RESPONSES

	Normal mode	LVRT mode	
Grounding resistance	10Ω	2Ω	0.8Ω
MAE of P (%)			
Proposed Method	0.02	0.02	0.03
Aggregated Method	0.54	0.91	0.74
MAE of Q (%)			
Proposed Method	0.02	0.01	0.02
Aggregated Method	0.48	0.88	0.69

V. CONCLUSION

This paper proposed a cyber-physical technique for dynamic modeling for wind farm considering the LVRT mode. The simulation results illustrate the proposed method can accurately estimate the dynamic behavior of wind farm, whether in LVRT mode or normal mode. Case studies demonstrate that the proposed method can take full advantage of the operating data

and improve the modeling accuracy of aggregation. This method not only solves the aggregation problem under the black-box system but also compensates for the errors occur in the aggregation process.

REFERENCES

[1] L. P. Kunjumuhammed, B. C. Pal, C. Oates and K. J. Dyke, "The adequacy of the present practice in dynamic aggregated modeling of wind farm systems," *IEEE Transactions on Sustainable Energy*, vol. 8, no. 1, pp. 23-32, Jan. 2017.

[2] J. Zou, C. Peng, Y. Yan, H. Zheng, and Y. Li, "A survey of dynamic equivalent modeling for wind farm," *Renewable Sustain. Energy Rev.*, vol. 40, pp. 956-963, 2014.

[3] S. Zhao and N.-K. C. Nair, "Assessment of wind farm models from a transmission system operator perspective using field measurements," *IET Renewable Power Gener.*, vol. 5, no. 6, pp. 455-464. 2011.

[4] Y. Zhang, E. Muljadi, D. Kosterev and M. Singh, "Wind power plant model validation using synchrophasor measurements at the point of interconnection," *IEEE Transactions on Sustainable Energy*, vol. 6, no. 3, pp. 984-992, July 2015.

[5] M. Liu, W. Pan, Y. Zhang, K. Zhao, S. Zhang and T. Liu, "A dynamic equivalent model for DFIG-based wind farms," *IEEE Access*, vol. 7, pp. 74931-74940, 2019.

[6] P. Wang, Z. Zhang, Q. Huang, N. Wang, X. Zhang and W. -J. Lee, "Improved wind farm aggregated modeling method for large-scale power system stability studies," *IEEE Transactions on Power Systems*, vol. 33, no. 6, pp. 6332-6342, Nov. 2018.

[7] Y. Zhao and J. V. Milanović, "Equivalent modelling of wind farms for probabilistic harmonic propagation studies," *IEEE Transactions on Power Delivery*, vol. 37, no. 1, pp. 603-611, Feb. 2022.

[8] H. R. Ali, L. P. Kunjumuhammed, B. C. Pal, A. G. Adamczyk and K. Vershinin, "A trajectory piecewise-linear approach to nonlinear model order reduction of wind farms," *IEEE Transactions on Sustainable Energy*, vol. 11, no. 2, pp. 894-905, April 2020.

[9] P. Wang, Z. Zhang, Q. Huang, N. Wang, X. Zhang and W. -J. Lee, "Improved wind farm aggregated modeling method for large-scale power system stability studies," *IEEE Transactions on Power Systems*, vol. 33, no. 6, pp. 6332-6342, Nov. 2018.

[10] J. He, L. Huang, D. Wu, C. Zhu and H. Xin, "*Frequency support from PMSG-based wind turbines with reduced DC-link voltage fluctuations*," CES Transactions on Electrical Machines and Systems, vol. 2, no. 3, pp. 296-302, Sep. 2018.

[11] J. J. Justo, F. Mwasilu, and J.-W. Jung, "Doubly-fed induction generator based wind turbines: a comprehensive review of fault ride-through strategies," *Renewable Sustain. Energy Rev.*, vol. 45, pp. 447-467, 2015.

[12] Q. Zhu, M. Ding, and P. Han, "Equivalent modeling of DFIG-based wind power plant considering crowbar protection," *Math. Problems Eng.*, vol. 2016, pp. 1-16, 2016.

[13] Y. Gao, Y. Jin, P. Ju, and Q. Zhou, "Dynamic equivalence of wind farm composed of double fed induction generators considering operation characteristic of crowbar," *Power Syst. Tech.*, vol. 39, no.3, pp. 628-633, 2015.

[14] M. Liu, W. Pan, Y. Zhang, K. Zhao, S. Zhang and T. Liu, "A dynamic equivalent model for DFIG-based wind farms," *IEEE Access*, vol. 7, pp. 74931-74940, 2019.

[15] Y. Jin, D. Wu, P. Ju, C. Rehtanz, F. Wu and X. Pan, "Modeling of wind speeds inside a wind farm with application to wind farm aggregate modeling considering LVRT characteristic," *IEEE Transactions on Energy Conversion*, vol. 35, no. 1, pp. 508-519, Mar. 2020.

[16] P. Chao, W. Li, X. Liang, S. Xu and Y. Shuai, "An analytical two-machine equivalent method of DFIG-based wind power plants considering complete FRT processes," *IEEE Transactions on Power Systems*, vol. 36, no. 4, pp. 3657-3667, July 2021.

[17] Y. Li, J. M. Guerrero, J. Yang, Y. Guan, G. Ma and J. Feng, "Dynamic equivalent modeling for black-box microgrid under multi-operating-point by using LSTM," *CSEE Journal of Power and Energy Systems*, early access, doi: 10.17775/CSEEJPES.2021.01660.

[18] C. Zheng et al., "A novel equivalent model of active distribution networks based on LSTM," *IEEE Transactions on Neural Networks and Learning*

Systems, vol. 30, no. 9, pp. 2611-2624, Sept. 2019.

[19] G. K. Venayagamoorthy, R. K. Sharma, P. K. Gautam and A. Ahmadi, "Dynamic energy management system for a smart microgrid," *IEEE Transactions on Neural Networks and Learning Systems*, vol. 27, no. 8, pp. 1643-1656, Aug. 2016.

[20] H. Shen, P. Tao, P. Zhao and H. Ma, "*Massive power device condition monitoring data feature extraction and clustering analysis using MapReduce and graph model*," CES Transactions on Electrical Machines and Systems, vol. 3, no. 2, pp. 221-230, Jun. 2019.

[21] Z. Zhang, S. Rao and X. Zhang, "*Performance prediction of switched reluctance motor using improved generalized regression neural networks for design optimization*," CES Transactions on Electrical Machines and Systems, vol. 2, no. 4, pp. 371-376, Dec. 2018.

[22] C. Mehdipour, A. Hajizadeh, and I. Mehdipour, "Dynamic modeling and control of DFIG-based wind turbins under balanced network conditions," *Int. J. Elect. Power Energy System.*, vol. 83, pp. 560-569, Dec. 2016.

[23] W. Li, P. Chao, X. Liang, J. Ma, D. Xu and X. Jin, "A practical equivalent method for DFIG wind farms," *IEEE Transactions on Sustainable Energy*, vol. 9, no. 2, pp. 610-620, April 2018,

[24] Y. Jin, D. Wu, P. Ju, C. Rehtanz, F. Wu and X. Pan, "Modeling of wind speeds inside a wind farm with application to wind farm aggregate modeling considering LVRT characteristic," *IEEE Transactions on Energy Conversion*, vol. 35, no. 1, pp. 508-519, March 2020.

[25] Z. Din, J. Zhang, Y. Zhu, Z. Xu and A. El-Naggar, "Impact of grid impedance on LVRT performance of DFIG system with rotor crowbar technology," *IEEE Access*, vol. 7, pp. 127999-128008, 2019.

[26] W. Li, P. Chao, X. Liang, Y. Sun, J. Qi and X. Chang, "Modeling of complete fault ride-through processes for DFIG-based wind turbines," *Renewable Energy*, vol. 118, pp. 1001-1014, April 2018.

[27] A. P. Gupta, A. Mitra, A. Mohapatra and S. N. Singh, "A multi-machine equivalent model of a wind farm considering LVRT characteristic and wake effect," *IEEE Transactions on Sustainable Energy*, vol. 13, no. 3, pp. 1396-1407, July 2022.

[28] J. Schmidhuber, "Deep learning in neural networks: An Overview," *Neural Networks*, vol. 61, pp. 85-117, Jan. 2015.

[29] M. Zhang, X. Wang, D. Yang and M. G. Christensen, "Artificial neural network based identification of multi-operating-point impedance model," *IEEE Transactions on Power Electronics*, vol. 36, no. 2, pp. 1231-1235, Feb. 2021.

Guiqing Ma was born in Nanyang, Henan Province, in 1997. He received the B.S. degree in electric automatization from Luoyang Institute of Science and Technology, Luoyang, China, in 2020. He is currently pursuing the M.S. degree in electric engineering at Shenyang University of Technology, Shenyang, China. His main research interests include wind turbine modeling, distributed control, and data-driven technique.
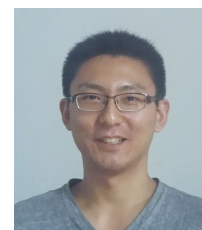
Yunlu Li received the B.S. in electronic information engineering from Shenyang University of Technology in 2009, the M.S. degree in control engineering in 2011 and Ph.D degree in power electronics and drives from Northeastern University in 2017, Shenyang, China. He is currently an associate professor in school of electrical engineering with Shenyang University of Technology, Shenyang, China. His research interests include data-driven based modeling technique for renewable energy system and nonlinear control theory for complex dynamic system.

Junyou Yang received the B.Eng. degree from the Jilin University of Technology, Jilin, China, the M.Sc. degree from the Shenyang University of Technology, Shenyang, China, and the Ph.D. degree from the Harbin Institute of Technology, Harbin, China. He was a Visiting Scholar with Department of Electrical Engineering and Computer Science, University of Toronto, Canada, from 1999 to 2020. He is currently the Head of the School of Electrical Engineering, Shenyang University of Technology. He is also a Distinguished Professor of Liaoning Province. His research interests include wind energy, special motor and its control.

Bing Wu was born in Tangshan, Hebei Province, in 1999. She received the B.S. degree in electrical engineering and automation from Jilin Institute of Chemical Technology, Jilin, China, in 2021. She is currently pursuing the M.S. degree in electric engineering at Shenyang University of Technology, Shenyang, China. Her main research interests include wind energy, distributed control, and smart grid.